Modelling of non-uniform corrosion-induced cover cracking in reinforced concrete

Santiago Guzmán , Jaime C. Gálvez and José M. Sancho

ABSTRACT

Cover cracking and spalling in concrete due to corrosion of reinforcement bars is one of the major concerns for durability of reinforced concrete structures and has been widely researched during recent years. Most approaches to the problem are based on a uniform corrosion and expansion pressure around the rebar.

However, corrosion rust tends to accumulate around the steel circumference that faces the concrete cover. From this outer part of the rebar, the corrosion front gradually advances to the inner, which entails a non-uniform expansive pressure around the rebar.

The purpose of the study is to simulate the effect of non-uniform rust distribution around the corroded rebar, taking advantage of an embedded cohesive crack finite element. The objective is to develop more realistic models for the estimation of the service life of reinforced concrete structures.

INTRODUCTION

Corrosion of reinforcement bars is one of the major reasons for deterioration of reinforced concrete (RC) structures. Oxidation of the reinforcement bars leads to the formation of rust which occupies a much greater volume than the original steel consumed by corrosion. Thus, tensile forces are generated in the surrounding concrete, with surface cracking eventually appearing.

Most approaches to the problem are based on a uniform corrosion and expansion pressure around the rebar. Such assumptions provide satisfactory results when modelling some laboratory accelerated corrosion tests (Andrade et al, 1993; Liu and Weyers, 1998; Bhargava et al, 2005; Chernin et al, 2010; Guzmán et al, 2011) and are generally accepted for the sake of simplicity.

However, a pitting or localised pattern represents the most common situation in concrete structures exposed to natural environments, especially regarding chloride-induced corrosion. The corrosion rust tends to accumulate around the steel

circumference that faces the concrete cover. From this outer part of the rebar, the corrosion front gradually advances to the inner, as chloride ions diffuse, which entails a non-uniform expansive pressure around the rebar. Although some recent studies have proposed elliptical or Gaussian distribution patterns (Liu and Li, 2004; Jang and Oh, 2010; Cao and Cheung, 2014; Du et al, 2014; Chen and Leung, 2015) for modelling, there is generally a lack of numerical simulation offered.

Therefore, the purpose of this study is to simulate the effect of non-uniform rust distribution around the corroded rebar. An embedded cohesive crack 2D finite element, as presented in previous work (Guzmán et al, 2012), is chosen here again in order to analyse the concrete fracture process. The objective is to develop more realistic models for the estimation of the service life of RC structures.

FINITE ELEMENT MODEL

Based on the so-called strong discontinuity approach (SDA), an embedded cohesive crack finite element (Sancho et al, 2007) is employed to model the non-linear fracture behaviour of concrete. In particular, a simple generalisation of the cohesive crack to mixed mode is used which assumes that the traction vector $\boldsymbol{t}$ transmitted across the crack faces is parallel to the crack displacement vector $\boldsymbol{w}$ (central forces model), i.e.:

$$\boldsymbol{t} = \frac{f(w)}{w}\boldsymbol{w}$$

where $f(w)$ is the classical softening function for pure opening mode (Figure 1). In order to avoid locking after a certain crack growth, the opportunity of crack adaptability within each element is provided, allowing the crack to adapt itself to the later variations in principal stress direction while its opening is small. Having exceeded a threshold value, the crack is considered consolidated and the crack direction becomes fixed. The finite element code FEAP (Taylor, 2013) is employed for numerical simulations. Plane strain formulation and the exponential softening curve are considered, assuming 100 N/m as the value of the specific fracture energy G_F.

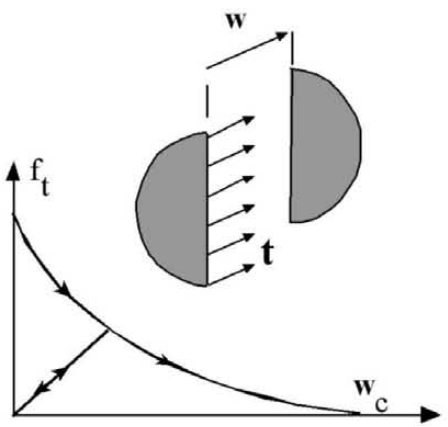

Figure 1. Softening curve for the cohesive crack model.

Regarding geometry, samples with a width of 150mm and with a middle side bar are considered, as indicated by Williamson and Clark (2000) who carried out experimental tests that will be compared with the present analysis results. Basic assumptions are the following:

1. Diameter of the bar, 16mm.
2. Cover depth-to-rebar diameter ratio (*c/d*) equals one.
3. Compressive strength of concrete f_c= 27.5/44.1 MPa. The corresponding Young's modulus is E_c= 24.8/31.4 GPa and tensile strength f_t= 1.83/2.55 MPa. In all cases, Poisson's ratio is ν_c= 0.2.
4. For the sake of simplicity, the mechanical properties of oxide products are taken to be the same as those corresponding to steel. In addition, a perfect sliding contact is chosen to reproduce the oxide-concrete interface.
5. Free boundary conditions are considered in order to reproduce the single rebar case found in the laboratory tests.

CRACKING PRESSURE OF CONCRETE COVER

From real RC structures exposed to an aggressive environment, oxide products around the rebar usually take a pseudo-elliptical shape, in such a way that the closer to the concrete surface, the more corrosion takes place. Figure 2 shows the most used analytical models for reproducing non-uniform corrosion, through patterns of theoretical free expansion of the rebar. The parameter α is defined as the ratio of maximum rust expansion of that corresponding to the uniform case when the total corrosion product is kept constant.

Following Jang and Oh (2010), a first approach to the problem would be based on the concept of cracking pressure, i.e. the internal pressure required to cause cracking of concrete cover due to reinforcement corrosion. That involves the aim of obtaining the value of the cracking pressure depending upon the different values of α.

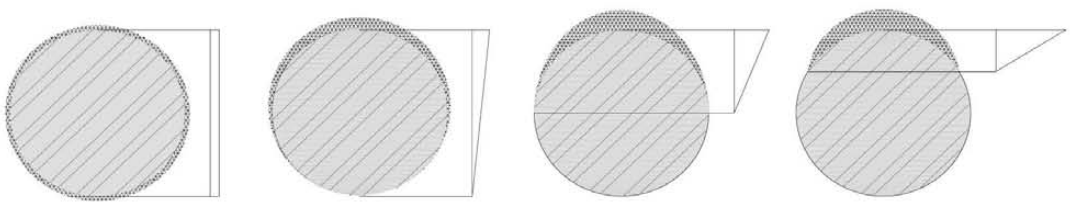

Figure 2. Different shapes of corrosion distribution in the reinforcement bar.

Contrary to the arguments offered by Jang and Oh (2010), in this case the reinforcement bar is considered explicitly in the finite element model. Conventional elastic parameters for steel are assumed (E_s= 210 GPa and ν_s= 0.3). Figure 3 depicts the pressure distribution acting on both steel and concrete boundary surfaces as a function of α value. Figure 4 and Table 1 summarise the resulting cracking pressures in terms of α value.

For comparison purposes, cracking pressure is equal to p_{max}, $p_{max}/2$ and $p_{max}/4$ when α= 2, 4 and 8, respectively, in order to obtain an equivalent average uniform pressure on concrete and take into account both the action and reaction forces.

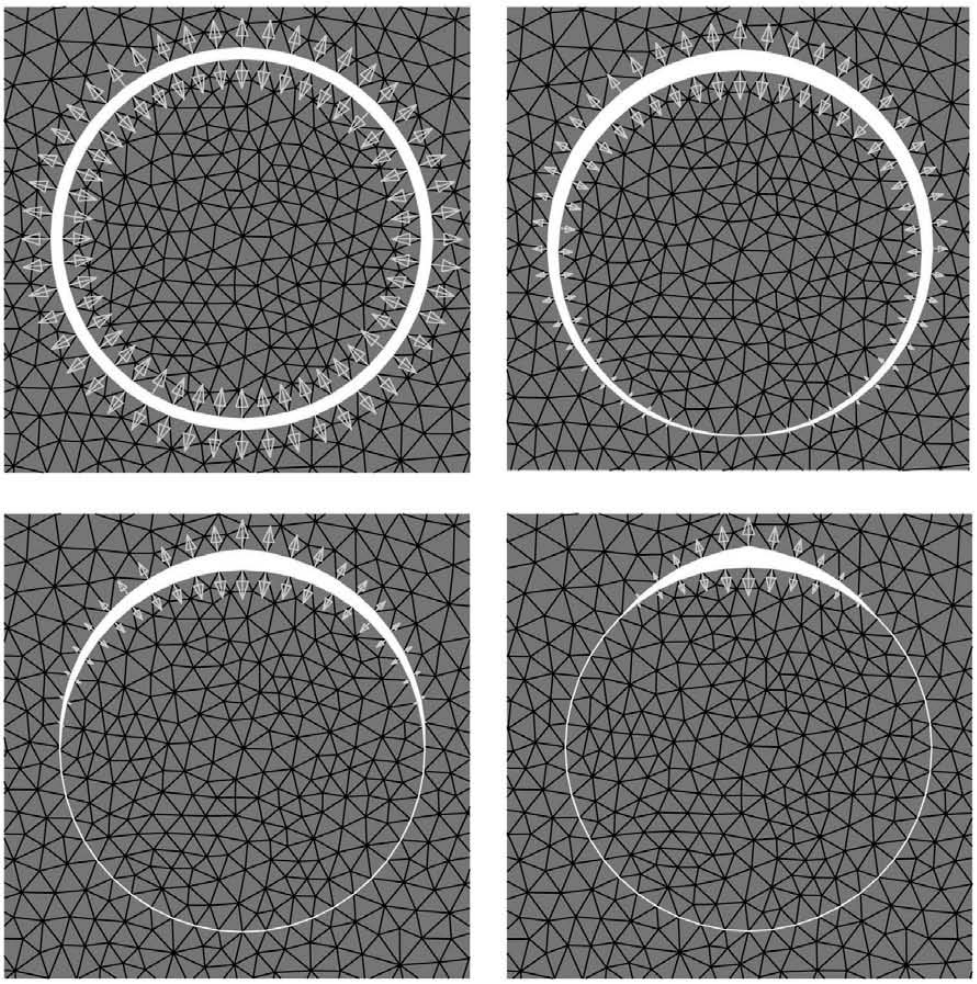

Figure 3. Pressure distribution around reinforcement bar (α= 1, 2, 4 and 8, respectively)

Two conclusions are derived: that cracking pressures clearly decrease as α value increases and that these strongly depend on tensile strength of concrete. The cracking pressure values obtained are similar to those found by Jang and Oh (2010), though some higher and experimental results provided by Williamson and Clark (2000) lead to greater cracking pressure for the uniform case (α= 1). This could be explained mainly because experimental tests are based on concretes with higher tensile strength ($f_t \approx$ 3.5 MPa). In addition, they are based on visual inspection of surface cracking and not when just the exact theoretical f_t value is reached at the concrete surface.

The effect of non-uniform corrosion over the first principal stress in concrete, when the first surface crack appears, is shown in Figure 5. In the bottom left corner of each diagram, nodal reactions on concrete inner boundary surface are also depicted.

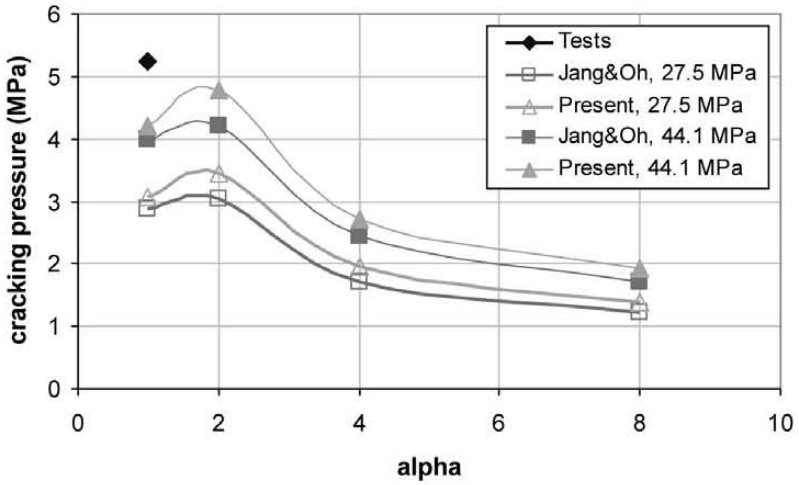

Figure 4. Cracking pressures as function of α. Please, see the text for references.

Table 1. Cracking pressures according to Figure 4 (MPa).

f_{ct} (MPa)	cover (mm)	A= 1	α= 2	α= 4	α= 8
27.5	16	3.1	3.4	2.0	1.4
44.1	16	4.2	4.8	2.7	1.9

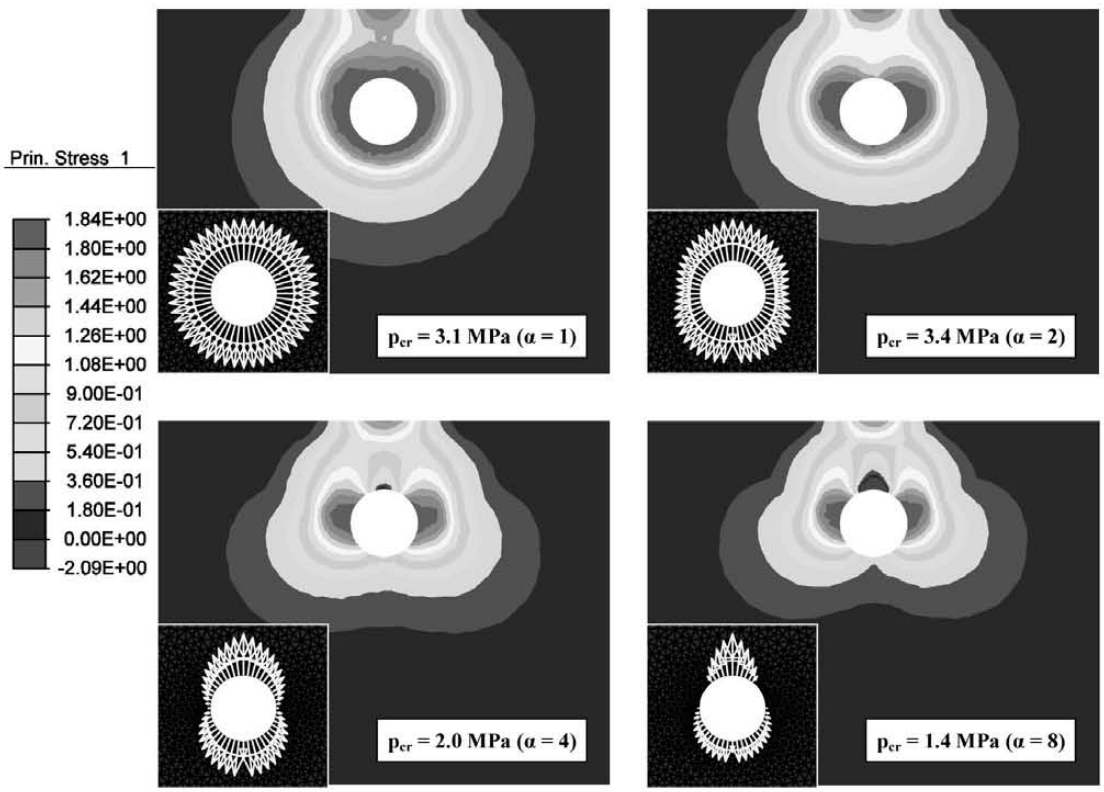

Figure 5. First principal stress and reactions in concrete under cracking pressure (MPa)

RUST EXPANSION

The next step is to introduce the effect of the rust expansion around the rebar, imposing displacement boundary conditions. Here, a fictitious increment of temperature in the rebar section will be used with a linear variation from 0 to ΔT_{max}, as shown in Figure 3. Then, the average ΔT_{avg} will be $\Delta T_{max}/2$, $\Delta T_{max}/4$ and $\Delta T_{max}/8$ when $\alpha = 2$, 4 and 8, respectively. A conventional $\varepsilon = 10^{-5}$ is taken as the steel thermal expansion coefficient.

If Δ represents the rebar radius increment due to free expansion of corrosion products for the uniform case and R_i is the initial radius (nominal) of the rebar, Δ comes from the following:

$$\Delta = \varepsilon R_i \Delta T_{avg}$$

Figure 6 shows the corresponding free expansion of the 16 mm reinforcement bar (the vertical displacements are shown in a different colour) that obtains the same corrosion product volume (corresponding to $\Delta = 1.6$ μm for the uniform case) but under different non-uniform cases. For the case $\alpha = 2$, taking $\Delta T_{max} = 2\ \Delta T_{avg}$, the same expansion unit volume is obtained directly. For the case $\alpha = 4$, a factor equal to $3\pi/8 \approx 1.18$ shall apply and, finally, for the case $\alpha = 8$, this factor is 1.56.

For comparative purposes, the same figures as those shown in the previous section are obtained (Figure 7 and Figure 8).

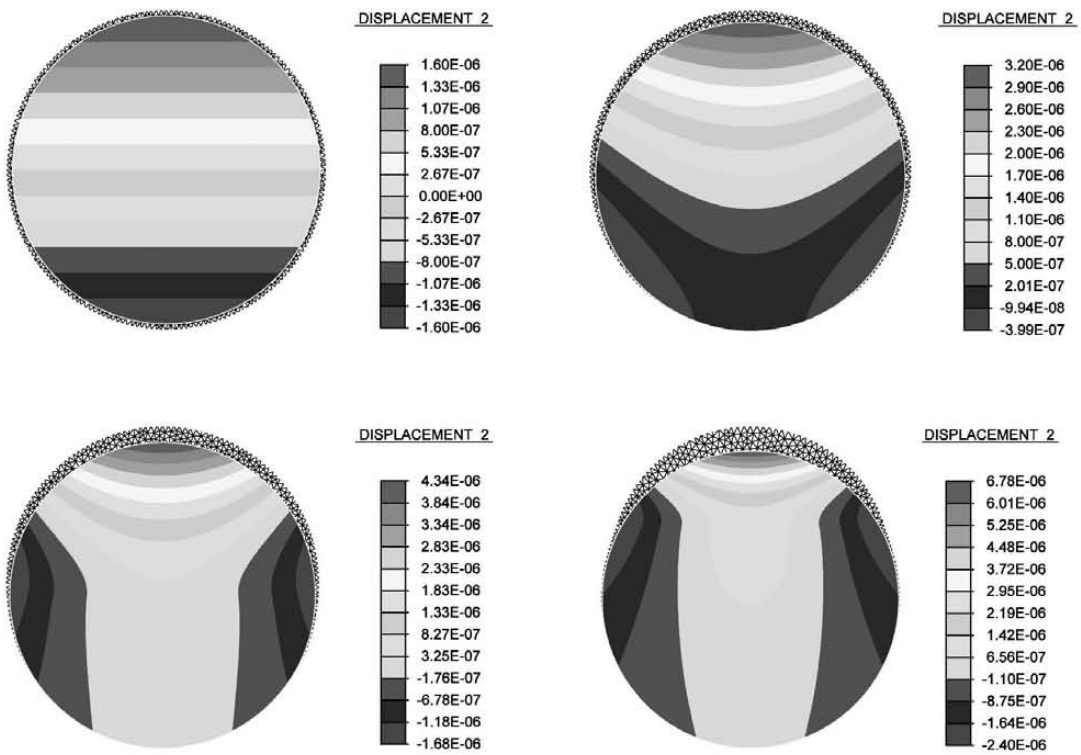

Figure 6. Free expansion of the reinforcement bar, $\Delta T_{avg} = 20^{o}C$ i.e. $\Delta_{avg} = 1.6$ μm ($\alpha = 1$, 2, 4 and 8, respectively).

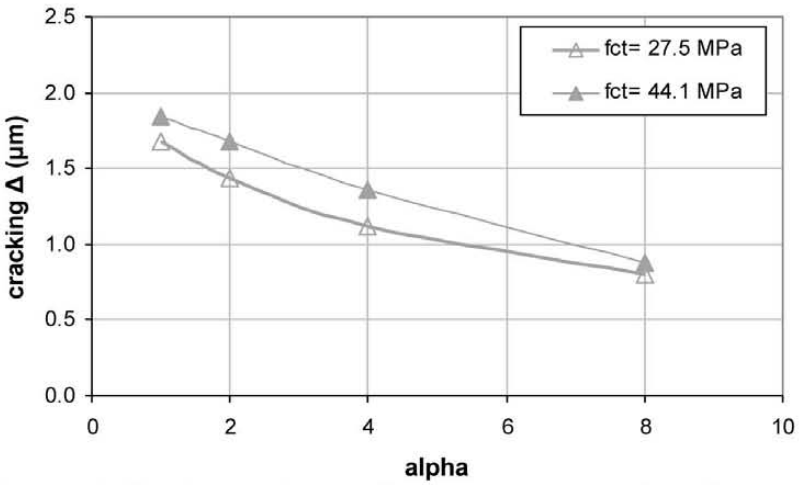

Figure 7. Cracking rebar radius increment as a function of α.

Table 2 Cracking rebar radius increment according to Figure 7 (μm)

f_{ct} (MPa)	cover (mm)	α= 1	α= 2	α= 4	α= 8
27.5	16	1.7	1.5	1.1	0.8
44.1	16	1.8	1.7	1.4	0.9

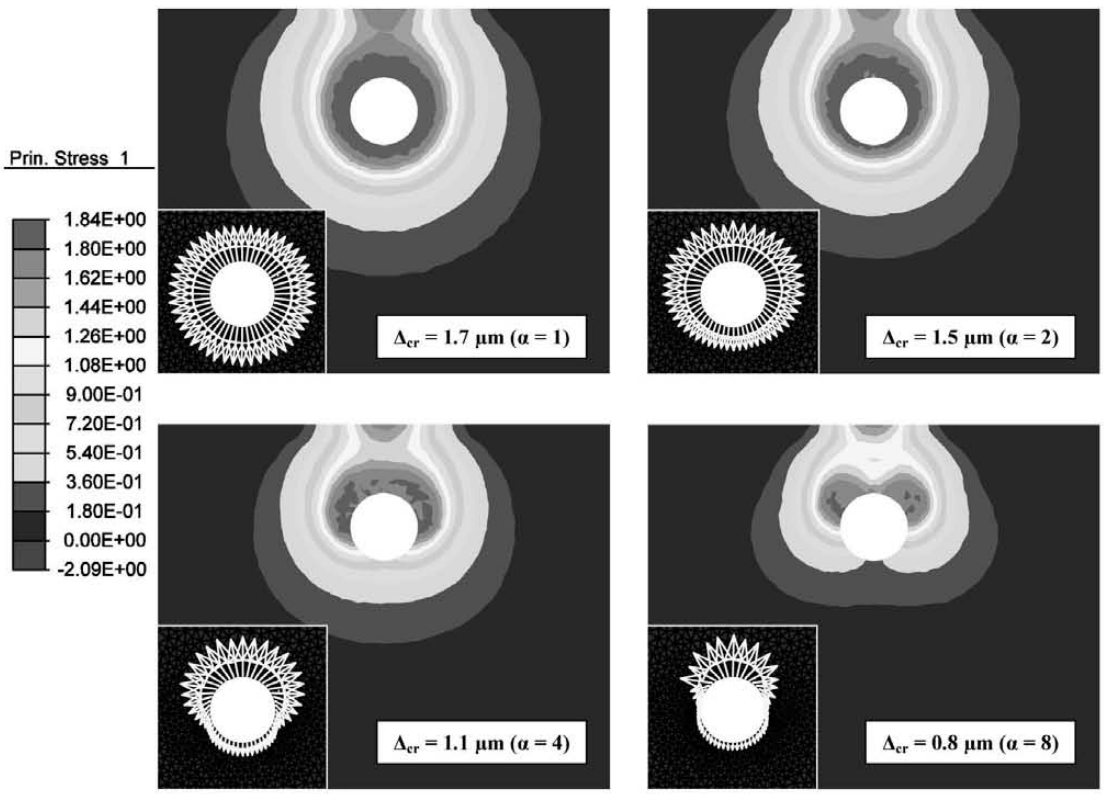

Figure 8. First principal stress and reactions in concrete under cracking rebar radius increment (MPa)

CONCLUSION

Taking advantage of an embedded cohesive crack finite element, the effects of non-uniform corrosion around a rebar on the surface cracking of concrete is explored under two approaches: imposed loads (cracking pressure) and displacements (rust expansion). Although the latter approach appears as a more realistic one, both do lead to a significant decrease of the corrosion amount needed to cause the concrete surface to crack when non-uniform corrosion is considered. As expected, the critical values depend on the compressive strength of concrete.

Further analysis would be required that considered certain other significant aspects, such as the influence of the ratio *c/d*, the determination of the rust mechanical properties and the penetration of these corrosion products in the microcracks of concrete.

ACKNOWLEDGEMENTS

The authors gratefully acknowledge the financial support provided by Ministry of Economy and Competitiveness of Spain by means of the Research Fund Project DPI 2011-24876.

REFERENCES

Andrade, C., Alonso, C., and Molina, F.J. (1993). "Cover cracking as a function of bar corrosion: part 1- Experimental test". *Mater. Struct.*, 26: 453-464.

Bhargava, K., Ghosh, A.K., Mori, Y., and Ramanujam, S. (2005). "Modeling of time to corrosion-induced cover cracking in reinforced concrete structures". *Cement Concrete Res.*, 35: 2203-2218.

Cao, C. and Cheung, M.M.S. (2014). "Non-uniform rust expansion for chloride-induced pitting corrosion in RC structures". *Constr. Build. Mater.*, 51: 75-81.

Chen, E., and Leung, C. (2015). "Finite element modeling of concrete cover cracking due to non-uniform steel corrosion." *Eng. Fract. Mech.*, 134: 61-78.

Chernin, L., Val, D.V., and Volkh, K.Y. (2010). "Analytical modelling of concrete cover cracking caused by corrosion of reinforcement". *Mater. Struct.*, 43(4): 543-556.

Du, X., Jin, L., and Zhang, R. (2014). "Modeling the cracking of cover concrete due to non-uniform corrosion of reinforcement." *Corros. Sci.*, 89: 189-202.

Guzmán, S., Gálvez, J.C., and Sancho, J.M. (2011). "Cover cracking of reinforced concrete due to rebar corrosion induced by chloride penetration". *Cement Concrete Res.*, 41: 893-902.

Guzmán, S., Gálvez, J.C., and Sancho, J.M. (2012). "Modelling of corrosion-induced cover cracking in reinforced concrete by an embedded cohesive crack finite element". *Eng. Fract. Mech.*, 93: 92-107.

Jang, B.S., and Oh, B.H. (2010). "Effects of non-uniform corrosion on the cracking and service life of reinforced concrete structures". *Cement Concrete Res.*, 40: 1441-1450.

Liu, Y., and Li, Y. (2004). "Mechanistic model and numerical analysis for corrosion damage in reinforced concrete". *Int. J. Fracture*, 126: 71-78.

Liu, Y., and Weyers, R. (1998). "Modeling the time-to-corrosion cracking in chloride contaminated reinforced concrete structures". *ACI Mater. J.*, 95(6): 675-681.

Sancho, J.M., Planas, J., Cendón, D.A., Reyes, E., and Gálvez, J.C. (2007). "An embedded crack model for finite element analysis of concrete fracture". *Eng. Fract. Mech.*, 74: 75-86.

Taylor, R.L. (2013). FEAP - A Finite Element Analysis Program, http://www.ce.berkeley.edu/projects/feap/.

Williamson S.J., and Clark, L.A. (2000). "Pressure required to cause cover cracking of concrete due to reinforcement corrosion". *Mag. Concrete Res.*, 52(6): 455-467.